Journal of Mining and Environment (JME) Vol. 16, No. 4, 2025, 1417-1435

Shahrood University of Technology

Journal of Mining and Environment (JME)

Journal homepage: www.jme.shahroodut.ac.ir

Iranian Society of Mining Engineering (IRSME)

Targeting of Porphyry Copper Mineralization Using a Continuous-based Logistic Function Approach in the Varzaghan District, North of Urumieh-Dokhtar Magmatic Arc

Mobin Saremi [1], Abbas Maghsoudi [1*], Reza Ghezelbash [2], Mahyar Yousefi [3], and Ardeshir Hezarkhani [1]

1. *Department of Mining Engineering, Amirkabir University of Technology, Tehran, Iran*
2. *School of Mining Engineering, College of Engineering, University of Tehran, Tehran, Iran*
3. *Faculty of Engineering, Malayer University, Malayer, Iran*

Article Info

Received 20 July 2024

Received in Revised form 5 August 2024

Accepted 30 August 2024

Published online 30 August 2024

DOI: 10.22044/jme.2024.14752.2803

Keywords

Porphyry copper deposit

Stream sediment geochemistry

Staged factor analysis

Geochemical mineralization probability index

MPM

Abstract

Mineral prospectivity mapping (MPM) is a multi-step and complex process designed to narrow down the target areas for exploratory activities in subsequent stages. To pinpoint promising zones of porphyry copper mineralization in the Varzaghan district, NW Iran, various exploration evidence layers were employed in alignment with the conceptual model of these deposits. These layers encompass fault density, proximity to intrusive rocks, multi-element geochemical anomalies, and distances to phyllic and argillic alterations. The geochemical anomaly maps, recognized as the most effective layers, were generated through staged factor analysis (SFA) and the geochemical mineralization probability index (GMPI). Other layers were weighted using a logistic function, and their values were transformed into 0 -1 interval. Ultimately, to integrate the weighted layers, the fuzzy gamma operator and the geometric average method were applied. The normalized density index and prediction-area (P-A) plot were employed to evaluate the MPM models. The findings indicate that the developed models possess considerable validity and can be effectively utilized for planning future exploration endeavors.

1. Introduction

Mineral exploration is inherently risky and expensive, requiring extensive research, geological investigations, and drilling. Sampling and data analysis are also a major factor leading to increasing uncertainty and rising exploration costs. Therefore, it is necessary to apply various exploration layers to recognize promising areas of mineralization, which enhance and improve the understanding of mineralization patterns. In other words, each exploration method has its advantages and disadvantages. Hence, combining exploration datasets derived from different sources such as geochemical [1], geophysical [2], and geological data [3] can dramatically increase the success in the exploration of undiscovered deposits [4]. In the primary stages of mineral explorations (known as the prospecting phase), mineral prospectivity mapping (MPM) can be adapted to reduce the areas covered by exploration operations [5]. MPM effectively integrates the results of different exploration layers to recognize promising areas [6-9]. The four major branches of MPM are knowledge-driven, data-driven, continuous (based on the logistic function), and hybrid methods. They aim to integrate the weighted evidence maps for prospective map construction [10-15].

Data-driven methods such as machine learning are widely used in geosciences [16-19]. In these methods for MPM, the locations and characteristics of the known mineral occurrences (KMOs) of the type sought in the study area are utilized for defining the "training dataset" [9, 20-22].

Corresponding author: a.maghsoudi@aut.ac.ir (A. Maghsoudi)

However, these methods therefore introduce exploration bias due to accessibility factors and exploration criteria as KMOs are used as training sites. Although these models can predict KMOs effectively, an essential question arises: How many KMOs in the study area are needed to sufficiently serve as training sites? In knowledge-driven MPM methods, there are exploration biases and uncertainties arising from expert judgment in the traditional discretization of continuous spatial values into some arbitrary classes. Indeed, these methods use the knowledge of multiple experts to determine the weights of the evidence maps [23, 24]. This leads to different results because experts' opinions differ based on various factors [25]. Other MPM methods can assign weights to the evidence layer using a hybrid method. When it comes to weighting relevant classes of evidence layers and integrating them, these methods have the same disadvantages as data- and knowledge-driven methods. To address these issues, researchers have proposed continuous weighting methods based on logistic functions [10, 26]. In these methods, the location of KMOs is not applied as training points and the evidence values representing mineralization are not discretized using arbitrary intervals, resulting in a significant decrease in uncertainties. For these reasons, this method was applied in this research.

Different layers are utilized for MPM, among them, the geochemical anomaly map is considered the most important [27-30]. At the regional scale for mineral exploration, geochemical data derived from stream sediment samples are typically used to examine the mineralization favorability of the area [31, 32]. To better understand the geochemical status of the study area, stream sediment data are mostly subjected to multivariate analysis methods such as staged factor analysis (SFA) to extract an anomalous geochemical signature linked to the mineral deposit-type sought. SFA is a statistical method that reduces a multivariate dataset to a few key factors endeavoring to find the hidden multivariate data structure. Therefore, SFA was utilized in this research to identify hidden relationships between geochemical elements and to produce an anomalous geochemical signature map. Subsequently, a logistic function called the geochemical mineralization probability index (GMPI) is then utilized to assign the optimal fuzzy weights. Due to this, assigning the appropriate weights to relevant classes of geochemical is a challenging issue. Modeling geochemical anomalies in stream sediment data presents another challenge because the materials of each stream sample come from upstream sources. Various methods are applied to map geochemical data from stream sediments. For example, methods such as the variety of interpolation techniques [26], sample catchment basin (SCB) mapping approach [33], point symbol maps and, weighted drainage catchment basin (WDCB) approach [34] can be mentioned. This study was conducted with two main objectives:

1- The identification of key multi-element geochemical signatures and the modeling of geochemical anomalies related to porphyry copper deposits through the utilization of interpolation and SCB methods.

2- Combining the obtained geochemical layers with other efficient exploration layers in the Varzaghan district northwest of Iran to achieve more accurate exploration targets of porphyry copper mineralization.

Finally, the normalized density (Nd) index and prediction-area (P-A) plot are utilized to evaluate the different MPM models based on the locations of KMOs. Figure 1 shows the stages of the research.

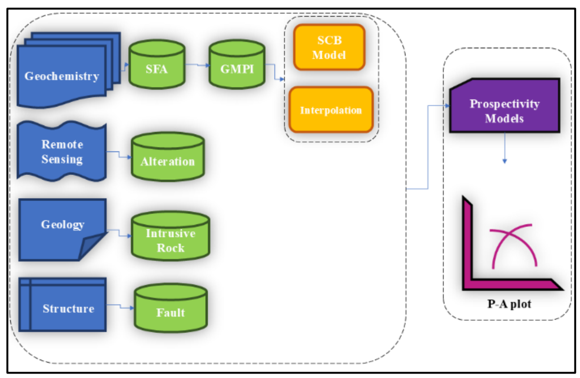

Figure 1. The multi-steps of MPM procedure in this research.

2. Geology of Varzaghan region

The Varzaghan area is situated in the northwest of the Cenozoic Urumieh–Dokhtar magmatic belt (UDMB), which is part of the collisional Alpine–Himalayan orogenic belt that extends from western Europe to Turkey and across Iran to western Pakistan [35, 36]. There are numerous porphyry copper mineralization within the UDMB, including two large deposits, namely the Sarcheshmeh and Sungun deposits, as well as dozens of medium- to small-scale deposits [37, 38].

The Varzeghan area consists of metamorphic rocks and a cover of Cretaceous rocks, especially in the northern part of the study area. The Cretaceous sequence contains reefal limestone, sandstone, marl, acidic to intermediate tuff and, andesitic lava flow [39]. Cenozoic rocks, covering extensive areas, comprise mainly porphyritic andesite, andesitic basalt, porphyritic dacite, trachyt, ignimbrite and, rhyolite that were intruded by acidic to intermediate stocks and dikes. The sub-volcanic intrusive rocks include granites, granodiorites, microdiorite and monzonite-micromonzonite of the Oligo-Miocene age. The mineralization and associated hydrothermal alteration were related temporally and spatially to the emplacement of these bodies [39, 40]. Quaternary intermediate volcanic rocks represent the youngest magmatic activity, succeeded by fluvial sediments and recent alluvium. The geological map of the studied area is presented in Figure 2.

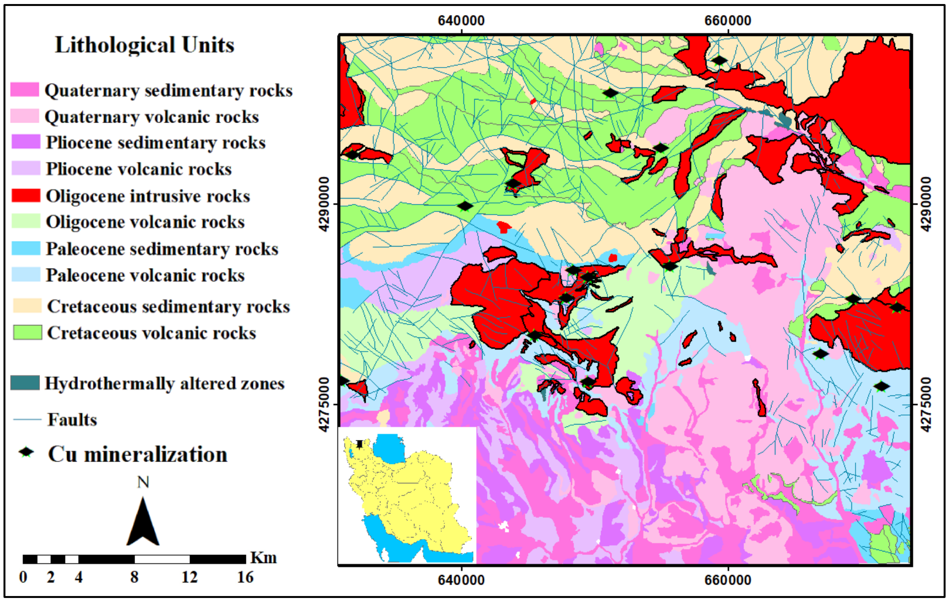

Figure 2. Geological map of Varzaghan district [41]

Porphyry copper deposits are hydrothermal systems characterized by distinct geological features and geochemical signatures. Leveraging these geochemical markers can significantly enhance the success rate in identifying exploration targets. In the study region, the intense activity of intrusive masses has led to the formation of porphyry copper mineralization and hydrothermal alteration [35, 42, 43]. Various granitoids, dating from the Oligocene to Miocene ages, play a critical role in the mineralization of Cu ± Au ± Mo porphyry deposits, Cu ± Au skarn deposits, and epithermal gold deposits. Notably, deposits with magmatic affinities in this area are predominantly associated with Oligo-Miocene intrusive bodies [41]. Previous research in this region has highlighted the geochemical association of Cu, Mo, Au, and Bi as key proximal indicators of porphyry copper deposits, meaning these elements are spatially and genetically linked to the deposits [33, 44]. Additionally, the presence of As and Sb is recognized as an important geochemical footprint for porphyry copper systems and can often be detected in their vicinity. By integrating the geochemical characteristics of porphyry copper deposits with insights from earlier studies, a strong geochemical signature can be effectively established. Studies focused on the region have identified that elements such as Ag, As, Au, Bi, Cu, Fe, Mo, Pb, Sb, and Zn are geochemically closely related to porphyry copper deposits. These elements serve as significant tracers and indicators, aiding in the exploration and identification of mineralization within the area [44, 45].

3. Materials:

3.1. Deposit model

MPM relies heavily on the creation of a conceptual model for target deposits. A conceptual model of a specific type of mineral deposit based on the KMOs serves as a guide for finding regions with the same characteristics. The information layers for MPM are selected according to the descriptive model of the target deposits. Thus, it is of utmost importance to create an accurate conceptual model with complete details. Based on studies conducted on porphyry copper deposits, the following features can be employed for MPM:

- These deposits are linked to subduction zones and are associated with intrusive rocks such as granodiorite, quartz diorite and, monzonite [46]. These deposits form in proximity to these intrusive rocks, representing a spatial and genetic relationship[47].
- During the formation of porphyry copper deposits, metal-rich fluids such as copper are transported through fractures and faults. These geological structures provide the necessary pathways and structural control for the movement of hydrothermal fluids [8]. Thus, the faults are one of the key factors in the exploration of porphyry systems around the world as well as in Iran.
- Based on geochemical studies conducted on porphyry copper deposits, these deposits were found to be associated with trace elements such as As, Au, Ag, Bi, Cu, Mo, Pb, Sb and, Zn or their halo in rocks, sediments and, soil [48]. By leveraging these elements, a significant multivariate geochemical signature can be developed to construct porphyry copper prospectivity models. As will be demonstrated in the following sections, utilizing this elemental data in conjunction with appropriate methods has resulted in the geochemical anomaly evidence layer generation as the most essential evidence layer in this region.
- Hydrothermal fluid processes can change the mineralogy and chemical composition of rocks in porphyry copper deposits [49]. As a result, these deposits are often associated with hydrothermal alteration zones, including potassic, argillic, phyllic, and propylitic alterations, which typically occur in patterns from the center outward [50]. The presence and extent of these hydrothermal alterations are commonly regarded as indicators of the scale and intensity of ore enrichment.

3.2. Stream sediment geochemical data

In 2012, a regional-scale geochemical survey was carried out in the Varzaghan area by the Geological Survey of Iran. As part of this exploration program, a total of 1067 stream samples were collected at a sampling density of one sample per 2 km^2. These samples were analyzed using inductively coupled plasma optical emission spectrometry (ICP-OES) and fire assay methods. The ICP-OES and fire assay methods were applied to analyze and determine 40 elements and Au, respectively. In this study, 10 trace elements (Ag, As, Au, Bi, Cu, Fe, Mo, Pb, Sb, and Zn) were utilized for further geochemical investigations. These elements are utilized in the exploration of hydrothermal deposits such as porphyry copper mineralization [40]. This study used data from 792 samples collected for geochemical studies. The locations of the collected samples are shown in Figure 3.

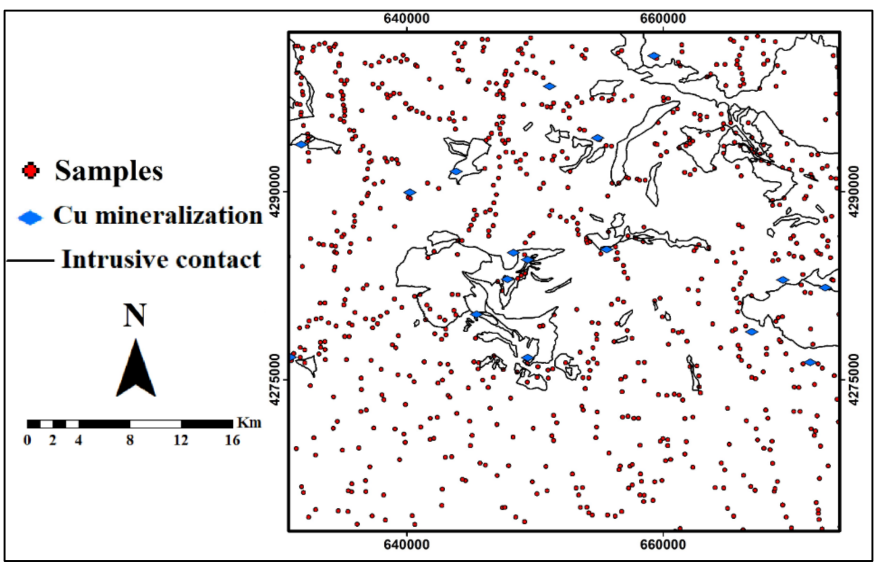

Figure 3. Stream sediment samples in Varzaghan region and their distribution

4. Methods:
4.1. Sigmoid logistic function

In MPM, exploration data is initially collected and processed based on the conceptual model of the target deposit [10]. Since these layers have different value ranges, they cannot be directly compared or used to create prospect maps [20]. To address this, the values of the evidence layers should be transferred to a new space, for example, 0-1 [25]. For this purpose, an optimized logistic function can be employed that does not rely on expert opinions to calculate parameters. Therefore, the exploration bias is significantly reduced because this function is not based on expert judgment.

$$F_E = \frac{1}{1+e^{-s(E-i)}} \quad (1)$$

where F_E is the value of the fuzzy membership, assigned fuzzy score, s, is the slope of the logistic function, i is the inflection point of the logistic function and E is weighted fuzzy evidence falling in the domain [0,1]. Also, the values of i and s are obtained from the equations 2 and 3, respectively:

$$i = \frac{E_{max} + E_{min}}{2} \quad (2)$$

$$s = \frac{9.2}{E_{max} - E_{min}} \quad (3)$$

4.2. Geometric average method

Various methods are used to combine the exploratory layers of evidence, one of them is the geometric average [51]. The geometric average for n values is defined as the n root of their product. This function is determined for a dataset using Equation 4:

$$G_A(V_1, V_2, \dots V_n) = \sqrt[n]{V_1 . V_2 \dots V_n} \quad (4)$$

Where V_n is the i^{th} evidential layer.

The geometric average method is used only for positive values. So, if the evidential layers have negative values, they must first be transferred to positive space [52]. The logistic function (Equation 1) can be used for this, which transfers the negative values into positive space.

4.3. Fuzzy Gamma

Fuzzy logic can be applied to integrate fuzzy evidence layers [53]. This logic is determined based on a membership function. It measures the degree to which a given element is a member of a set. The membership function can take any value between 0 and 1. To create a prospectivity map for detection exploration target zones for further exploration, fuzzy MPM combines fuzzy evidence maps. For integration, various fuzzy operators can be used to integrate the fuzzy evidence layers. In this regard, any existing fuzzy operator can be utilized, taking into account the type of mineralization sought and the purpose of the integration. The fuzzy gamma operator was used to integrate weighted evidence maps in this study. This operator is defined using the fuzzy algebra product and the fuzzy algebra sum by the following representation:

$$\mu_{combine} = (\prod_{i=1}^{n} \mu_i^{1-y}) \times (1 - \prod_{i=1}^{n} (1-\mu_i)^{y}) \quad (5)$$

where γ is a parameter chosen in the range (0, 1). When γ is 1 the combination is the same as the fuzzy algebraic sum, and when γ is 0 the combination is equal to the fuzzy algebraic product.

4.4. SFA

The multi-element geochemical layer is one of the most important layers in the MPM [54, 55]. The use of regional-scale stream sediment geochemical data plays a crucial role in comprehending the migration patterns of various elements and identifying promising areas for further exploration [34, 56, 57]. Stream sediments contain extensive mineralization information and may form geochemical secondary halos [58]. Accordingly, geochemical anomalies identified in stream sediments are considered important geochemical indicators and are one of the most effective tools for regional geochemical studies [59]. Processing the geochemical data always faces challenges due to its complex nature [60]. Thus, before modeling the geochemical anomalies, some statistical techniques must be carried out. Statistical methods include several univariate and multivariate (Such as PCA-FA-MAD-$\bar{X} \pm tS$) methods. Multivariate statistical methods can provide better results than univariate methods due to the intensification of multi-element geochemical halos [61, 62]. One of the most widely used multivariate statistical methods is factor analysis (FA), which has been frequently used by many researchers for processing geochemical data and identifying promising areas [63, 64]. This method can reveal the hidden structure between the chemical elements by reducing the dimensions of the data into several factors with appropriate quality [63]. Despite the widespread use of FA, this method still presents challenges. One of the most important questions is how many representative factors to extract and which elements to represent in each factor? In addition, FA utilizes the entire data matrix, so the presence of chemical elements unrelated to mineralization can introduce noise and cause factor values to deviate greatly from actual values. To solve the mentioned problems, Yousefi et al.(2014) proposed SFA[65]. This methodology is used to categorize and reduce the number of geochemical variables and determine the paragenesis of ore elements step by step [61]. This method applies a combination of variables rather than a single variable. This can increase the probability of detecting of geochemical halos around the ore body and identifying anomalies associated with mineralization. In addition, the impact of random errors can be reduced by using multi-element. Principal component analysis and varimax rotation were utilized to extract the relevant factors and rotation in the SFA. In addition, factors with eigenvalues greater than 1 are retained. Finally, the elements with thresholds ≥ 0.6 within each factor are considered efficient.

4.5. GMPI

In some cases, multiple mineralization-related factors are identified at the end of the SFA, raising the issue of which factor or factors should be used as representative of mineralization. Using one factor and ignoring others can result in the loss of valuable information, which may ultimately lead to the loss of some important exploration targets. To address this issue, Yousefi et al. (2012) introduced the GMPI, a new method for continuous weighting of geochemical layers[26]. The GMPI is a powerful method to assign appropriate fuzzy weight to stream sediment geochemical data, enhancing the detailed identification of geochemical anomalies [26, 66, 67]. This index is determined by using a logistic function and converting the obtained factor values into the range [0-1]. Compared to linear transformations, the logistic function provides clearer and more distinct boundaries for the separation and classification of different communities. Figure 4 shows the comparison of the transition to 0 and 1 between nonlinear (logistic) versus linear transformations. To calculate the GMPI, the logistic function has been used to fuzzify the factor score of each sample as follows:

$$GMPI = \frac{e^{Fs}}{1 + e^{Fs}} \tag{6}$$

4.6. Prediction-area (P-A) plot

In the various MPM approaches, each layer of evidence is generated from a specific exploration dataset (or source) and the role of each layer is different in the formation of a mineral deposit. Therefore, it is necessary to examine whether each evidence map can demonstrate the potential for a specific type of mineralization. In this regard, Yousefi et al. [68] developed the P-A plot, in which the percentage of KMOs (prediction rate) expected by prospect classes and the occupied areas of the corresponding prospect classes is helpful to quantify the relative importance of different prospect models. Moreover, the P-A plot can be applied to evaluate the performance of different prospectivity models. This process creates two curves, the intersection of which is an evaluation criterion [69]. Also, based on the parameters obtained from the P-A plot, it is possible to calculate the Nd, which is a criterion for evaluating various maps [70].

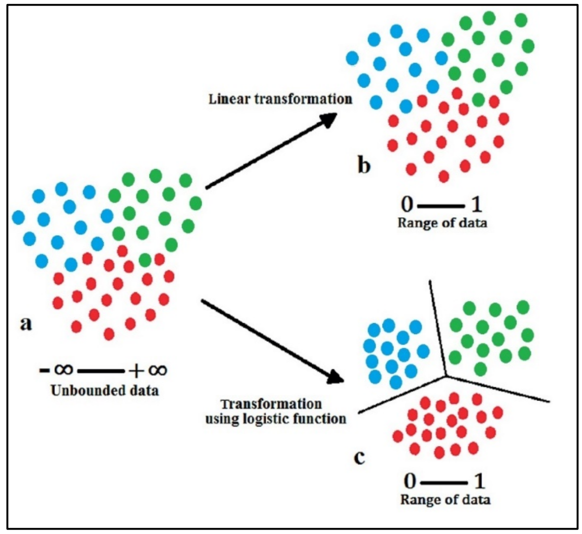

Figure 4. Schematic illustration of the comparison between logistic transformation and linear transformation for classification of different geochemical communities [65].

5. Results:

5.1. Weighted evidence layers

Based on the conceptual model for porphyry copper deposits and the available dataset from the Varzaghan district, this study considered four targeting criteria and five weighted layers of evidence to create a Cu-porphyry prospectivity map. These criteria include the multivariate geochemical signature, the geological and structural map, and the hydrothermal alterations criteria. To create the Cu-porphyry prospectivity maps, the spatial evidence values of the five layers (multi-element geochemical layer of SFA, geological layer of granodiorites, fault density layer and, alteration layers of phyllic and argillic) were transformed into a fuzzy range using logistic function.

5.2. Geochemical layer

Before applying the SFA method, the distribution of the geochemical data must be approximated to a normal distribution. The common approach for this work is a logarithmic transformation based on Natural (or Napierian) Logarithms (so-called Ln). The SFA was used to extract important factors based on the concentration data of 10 ln-transformed elements. Principal component analysis (PCA) was utilized to extract factors based on the concentration data of 10 elements, and also Varimax rotation of factors was applied. In the first step, FA scores greater than 0.6 were selected (Table 1). Pb, Fe and, Ag were discarded in this stage, as shown in Table 1. In the second stage, Zn was removed (Table 1). Therefore, the FA was repeated and two final factors were created. The factors created in this step are called clean factors. Factor 1 shows the aggregation of Au-Cu-Mo-Bi elements and factor 2 shows the aggregation of Sb-As, which can be suitable traces for identifying porphyry copper deposits in this area. Figure 5 shows the factor plot in rotational space as a more detailed representation of extracted factors.

Table 1. The values of factor score in the SFA method for the first, second and third steps

SFA									
First step				second stage			Third stage		
element	**F1**	**F2**	**F3**	**element**	**F1**	**F2**	**element**	**F1**	**F2**
Zn	-0.078	0.247	0.820	Zn	0.178	0.382	Cu	0.869	0.168
Pb	0.359	0.104	0.566	Cu	0.867	0.182	As	0.193	0.906
Ag	0.352	0.328	0.599	As	0.175	0.891	Sb	0.246	0.888
Cu	0.854	0.100	0.241	Sb	0.226	0.882	Au	0.641	0.443
As	0.233	0.860	0.093	Au	0.636	0.437	Mo	0.870	0.161
Sb	0.264	0.856	0.133	Mo	0.866	0.180	Bi	0.770	0.242
Au	0.658	0.395	0.155	Bi	0.760	0.273	Var	43.581	31.963
Mo	0.826	0.188	0.164	Var	37.099	29.265	Cum.Var	43.581	75.544
Fe	0.248	-0.156	0.516	Cum.Var	37.099	66.364			
Bi	0.711	0.268	0.176						
Var.	27.945	19.469	17.837						
Cum. var.	27.945	47.439	65.275						

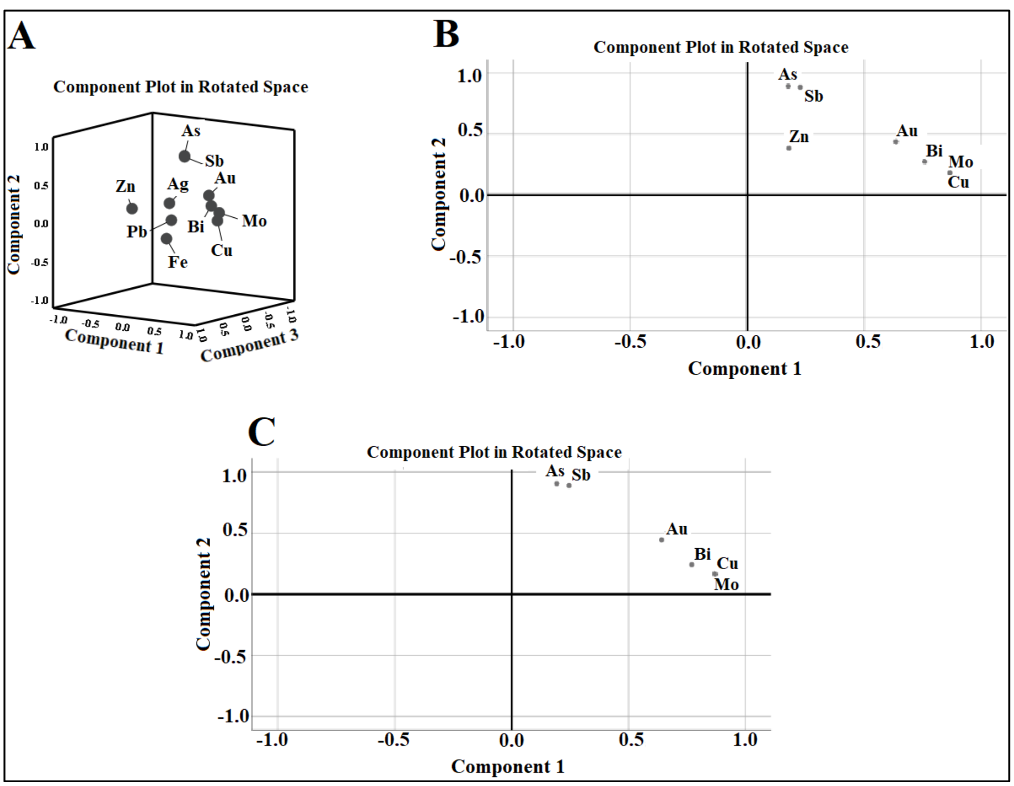

Figure 5. Component plots in rotated space in A) first, B) second and C) third step of SFA

From Table 1 it can be seen that both factors presented in the third step of the SFA contain important exploratory information. Therefore, both of them can be used as geochemical representatives to explore porphyry copper deposits in this area. A logistic sigmoid function called GMPI was used to generate a fuzzy layer of geochemical signatures for the deposit type sought. Then, using Equation 7, the desired processing was performed. After processing the results to model the geochemical data, the inverse distance weighted (IDW) and SCB methods were utilized (Figure 6).

$$\text{GMPI(porphyry Cu)} = \begin{cases} GMPI_{Cu-Au-Mo-Bi} \text{ if } GMPI_{Cu-Au-Mo-Bi} >= 0.72 \text{ and } GMPI_{As-Sb} < 0.71 \\ GMPI_{As-Sb} \text{ if } GMPI_{As-Sb} >= 0.71 \text{ and } GMPI_{Cu-Au-Mo-Bi} <= 0.72 \\ \text{Average } (GMPI_{Cu-Au-Mo-Bi}, GMPI_{As-Sb}) \text{ if } GMPI_{Cu-Au-Mo-Bi} >= 0.72 \text{ and } GMPI_{As-Sb} >= 0.71 \\ \text{Average } (GMPI_{Cu-Au-Mo-Bi}, GMPI_{As-Sb}) \text{ if } GMPI_{Cu-Au-Mo-Bi} <= 0.72 \text{ and } GMPI_{As-Sb} <= 0.71 \end{cases} \quad (7)$$

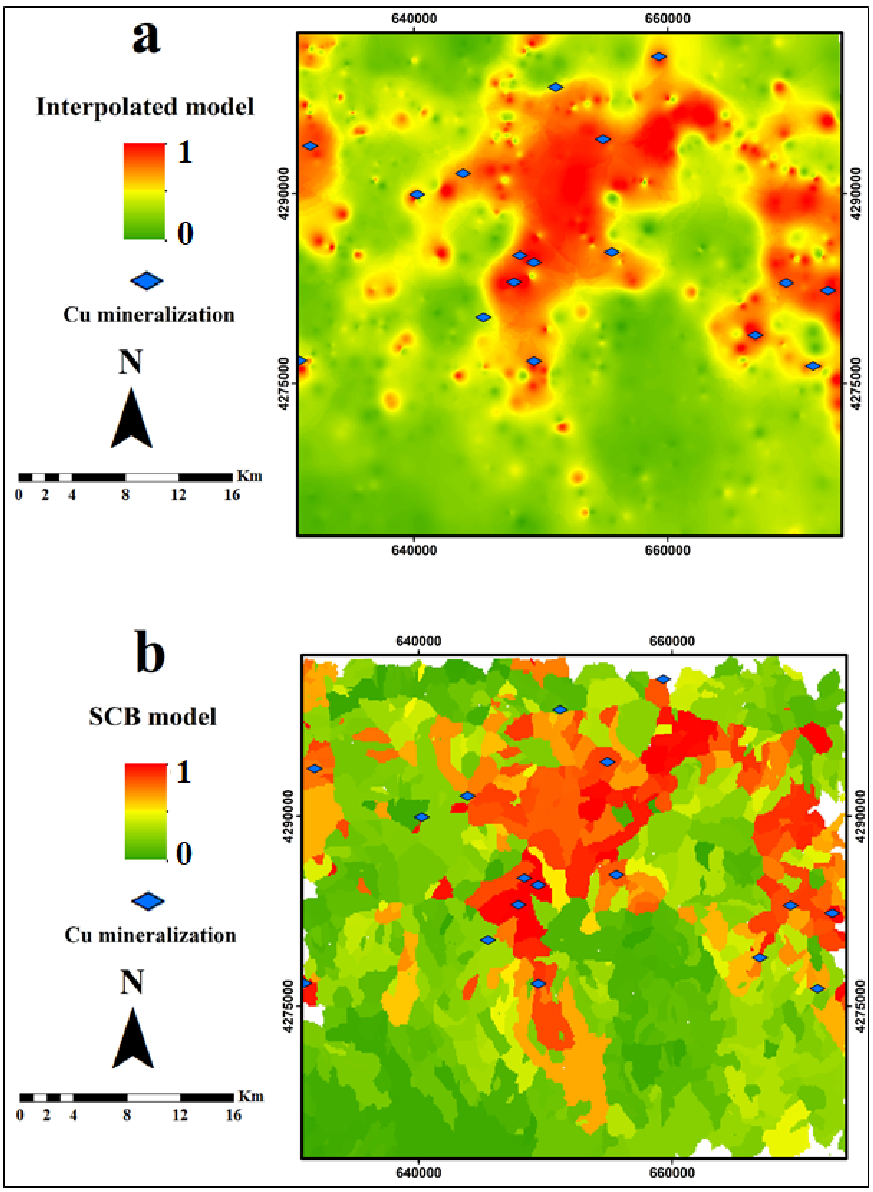

Figure 6. GMPI values converted from F1 and F2 factor scores obtained in the third step of the SFA accompanied by KMOs locations a) interpolated model b) SCB model.

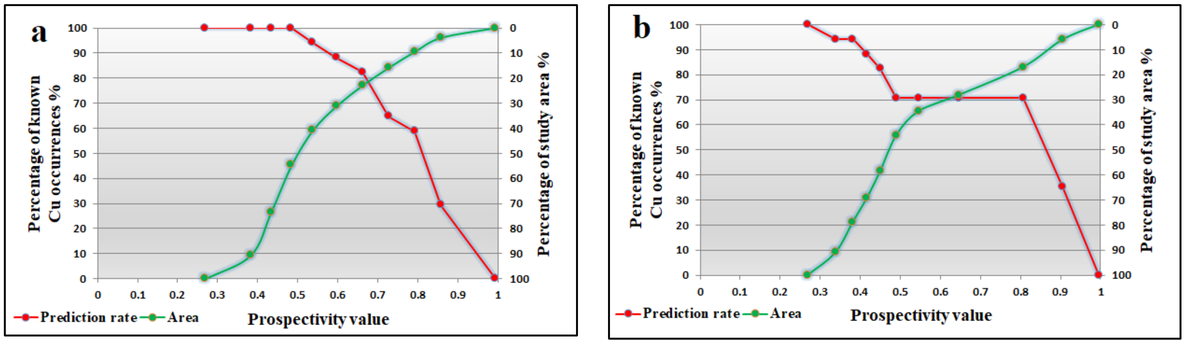

Figure 7. P-A plot for GMPI map a) interpolated model b) SCB model

The criterion for assessing and comparing the ability of the predicted rate of geochemical evidence layers is an intersection point between two curves in Figures 7a and 7b. If an intersection point appears at a higher location on the P-A plot for a model, it means that there are more mineral deposits in a smaller area of the model. Therefore, it is easier and more reliable to find the type of undiscovered reserves in a model that has higher prediction rates. The risk of identifying exploration targets is reduced by decreasing the area of promising regions and simultaneously increasing KMOs in these districts. For example, even if the area of the prospective area is reduced by just a few square kilometers, this can prevent an error in defining a geochemical project at a scale of 1:5000, which is approximately a few kilometers. According to the obtained curves, the intersection point of the P-A plot for the IDW model (Figure 7a) is drawn higher than the intersection point of the P-A plot for the SCB model (Figure 7b). Based on the intersection points in Figures 7a, 79% of the KMOs are delineated in 21% of the study area as shown in Figure 6. (a) interpolated model. In the SCB model, 72% of KMOs are identified in 28% of the studied area (Figure 7b). The observed improvement in the IDW model can be attributed to several factors, with sampling density being one of the most significant. In regions with high sampling point density, interpolation methods such as IDW may be more effective due to their dependence on sample density. Higher sampling density provides a more accurate representation of spatial patterns, reducing the likelihood of interpolation errors or over-smoothing that can occur in areas with sparse data. This detailed representation is crucial for generating models that accurately reflect regional heterogeneity, especially in complex geological settings where mineralization patterns may be highly localized.

5.3. Fault density (FD) layer

Structural controls play a significant role in the formation of mineral deposits. One of the major criteria for the formation and existence of hydrothermal deposits such as porphyry copper is the presence of structural systems [8]. Faults facilitate the passage of magma and the circulation of hydrothermal fluids. Thus, faults can be a suitable place for the exploration of all types of mineral deposits, especially those related to metals, and there are such structural geological features that indicate permeability. Regions with a high density of faults or places where faults intersect represent promising areas for porphyry copper deposits. These faults were extracted and digitized from the Varzaghan geological map at a scale of 1:100,000. Thus, the fuzzified FD layer was created to be contributed in MPM (Figure 8). The intersection point of the P–A plot for the fuzzified prospectivity model (Figure 9) shows 58% of the mineral occurrences predicted in 42% of the studied area.

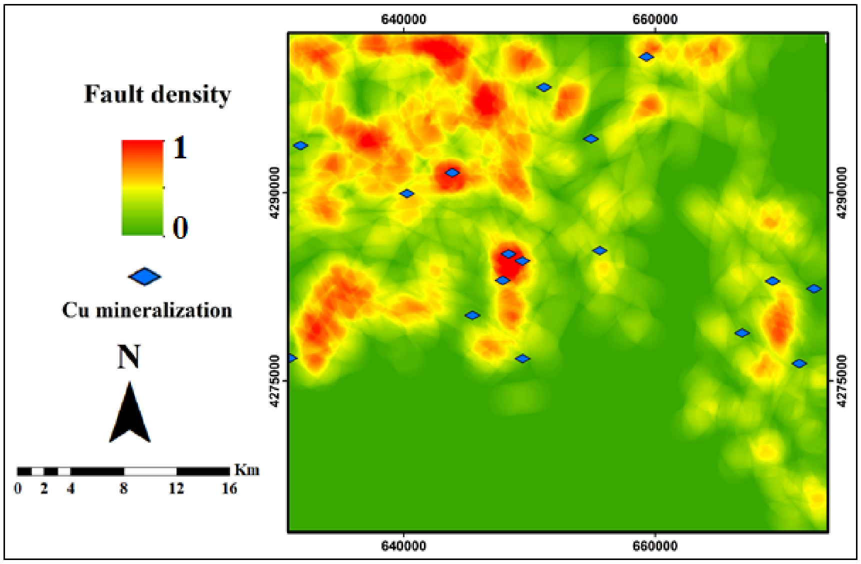

Figure 8. fault density layer of the studied area

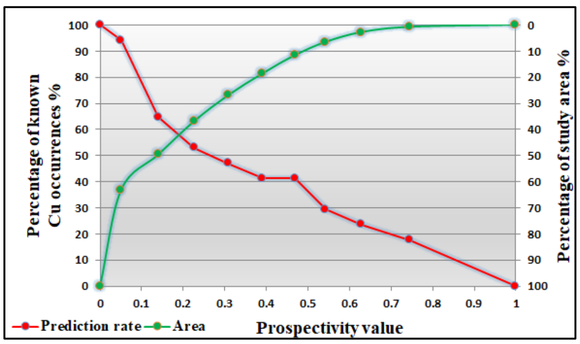

Figure 9. P-A plot for fault density layer

5.4. Geological layer

The 1:100,000 scale geological map of Varzaghan was created by GSI. This map is useful for extracting rock units related to porphyry copper deposits. The porphyry copper deposits on the UDMB are genetically and spatially related to the Oligo-Miocene intrusive rocks, which means that areas close to these rocks have a higher probability of porphyry copper mineralization than more distant areas. Hence, as part of this study, a weighted map of the distance to the intrusive rocks was created (Figure 10). After generating a weighted map of the distance to the intrusive rocks, the locations of KMOs in the study area were used as testing points in a P–A plot to evaluate it. Therefore, based on the intersection in Figure 10, 70% of the KMOs are predicted in 30% of the study area.

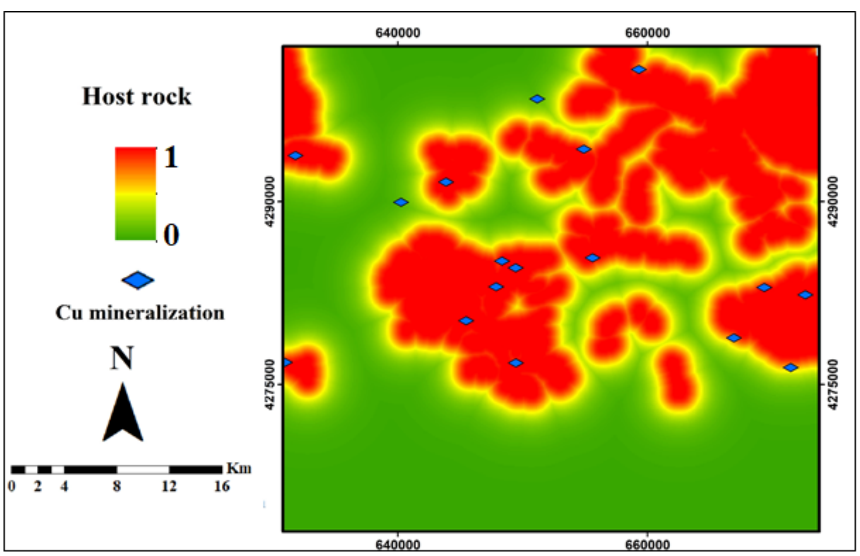

Figure 10. Distance to the intrusive rocks map.

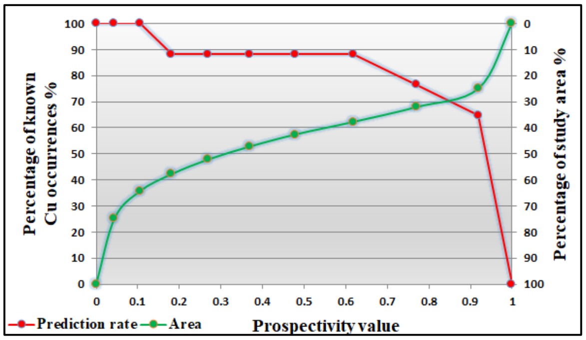

Figure 11. P-A plot for distance from the intrusive rocks

5.5. Hydrothermal alteration layers

Hydrothermal fluid processes can change the mineralogy and chemical composition of rocks leading formation of hydrothermal alterations [49]. Porphyry copper deposits are often associated with hydrothermal alteration zoning that includes potassic, argillic, phyllic and, propylitic alteration[50]. The presence and extent of hydrothermal alterations are often indicators of the scale and intensity of ore enrichment. Therefore, areas of phyllic and argillic alterations were identified using Aster images in this study. The maps of distance these two alterations were then created and their values were transferred into the fuzzy space using the logistic function of Equation 1 (Figure 12). According to Figure 12, it can be seen that the locations of KMOs display high association with phyllic and argillic alterations. One main reason can be the presence of intrusive rocks as well as many volcanic rocks in the region. Based on the intersection point in Figure 13a for the distance to argillic alteration, 75% of the KMOs are predicted in 25% of the study area whereas based on the intersection in Figure 13b for the distance to phyllic alteration, 71% of the KMOs are predicted in 29% of the study area. The P-A plot relevant to these alteration maps shows that the alteration layer of argillic (Figure 12a) demonstrated a higher prediction rate than that of phyllic alteration (Figure 12b).

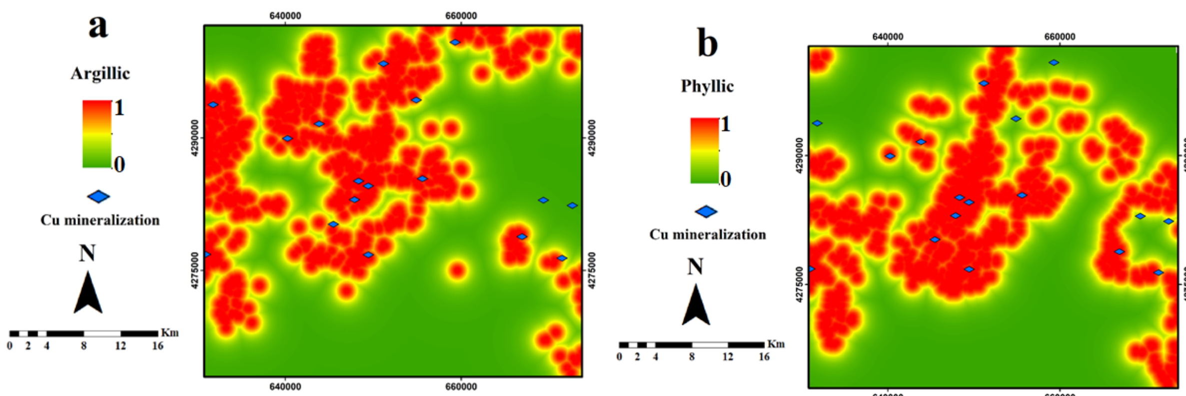

Figure 12. Alteration maps of the distance to a) argillic and b) phyllic in the study area.

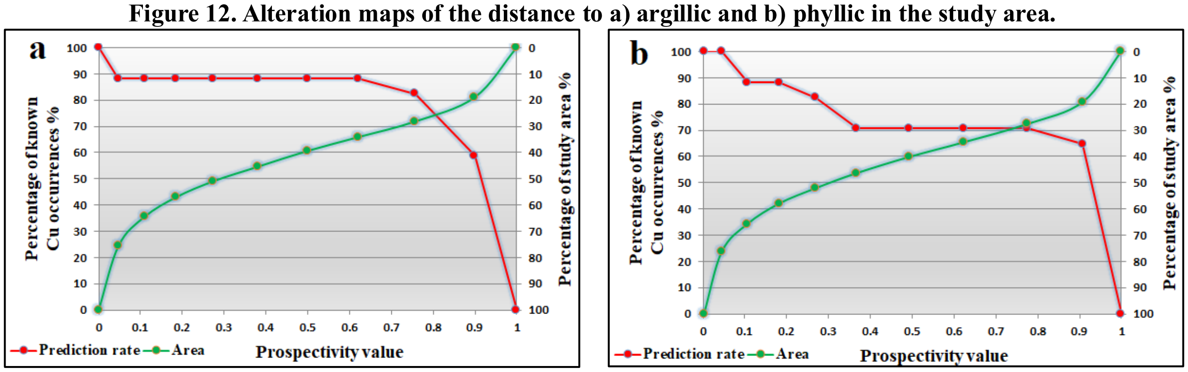

Figure 13. P-A plot for distance to a) argillic b) phyllic alterations.

6. Cu-porphyry prospectivity mapping

Several mathematical functions can be utilized to integrate the fuzzy evidence layers. For comparison, we used the geometric average method and the fuzzy gamma operator in this study. These two methods are relatively simple and easy to implement in the GIS framework. In addition, these methods do not use the location of KMOs, so the uncertainty of exploration can be reduced.

Therefore, the locations of 17 KMOs were only utilized to evaluate the prediction rate of MPM maps. In this research, first, the existing layers were combined using the geometric average method and their P-A plot was created (Figures 14 and 15). The same layers were then combined using the fuzzy gamma operator (Figures 16 and 17) and the results obtained using this method were compared with the geometric average method. From the P-A plots obtained for the four models constructed (Figures 15 and 17), it can be seen that almost all four models had relatively good predictions. Among these four models, the model made by fuzzy gamma using the interpolation map of geochemistry, fault density, distance to intrusive rocks, and distance to phyllic and argillic alterations has a higher prediction rate than other models (76%). In addition to the P-A plot, the N_d index was also used to evaluate the produced models. The parameters of the intersection point of the two curves (i.e. prediction rate and occupied area) were extracted from the P-A plot and used to calculate the N_d. Values greater than 1 indicate that the model is appropriate. In Figure 18, the N_d for all models obtained in this research and also for the layers used for integration are given. Based on the calculated parameters, the value of N_d for model produced by the fuzzy gamma using the interpolation map of geochemistry, fault density, distance to intrusive rocks and distance to phyllic and argillic alterations were determined to be 3.16, indicating that this model performs well in terms of predicting mineral deposit locations. It can be seen that models produced by the fuzzy gamma operator have a higher prediction rate than other models produced by the geometric average.

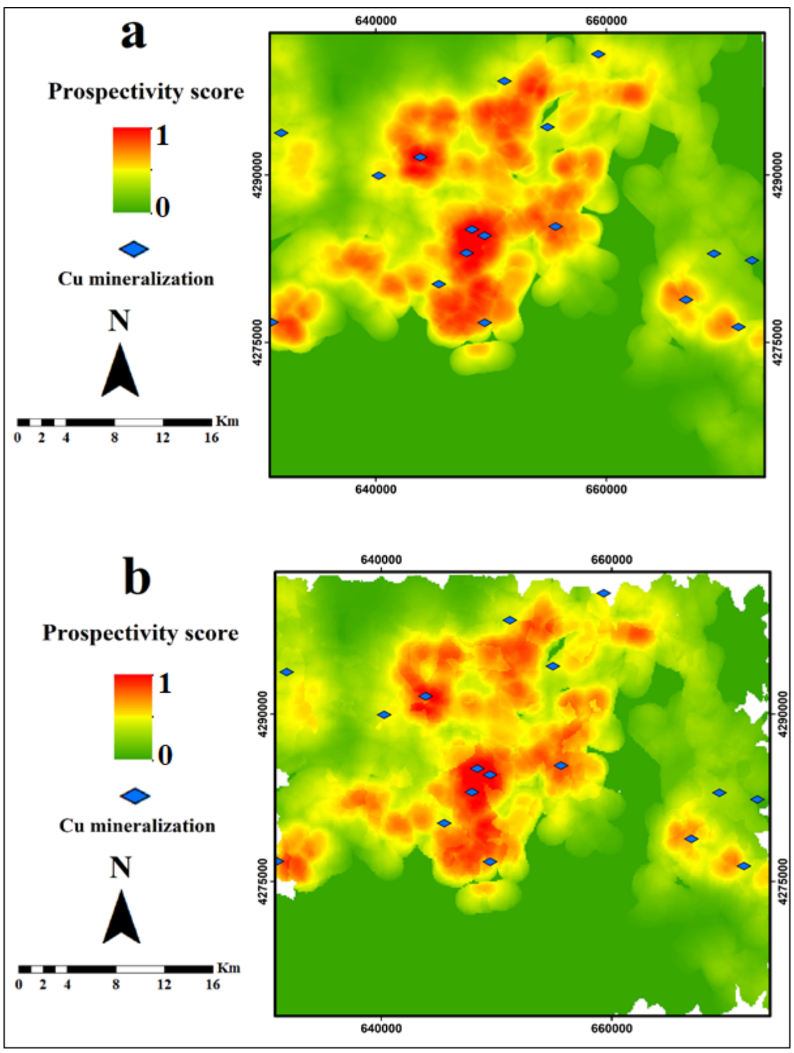

Figure 14. Mineral prospectivity model produced by combination of a) interpolated values of GMPI, fault density, distance to intrusive rocks and distance to argillic and phyllic alterations; b) SCB model of GMPI, fault density, distance to intrusive rocks and distance to argillic and phyllic alterations using geometric average

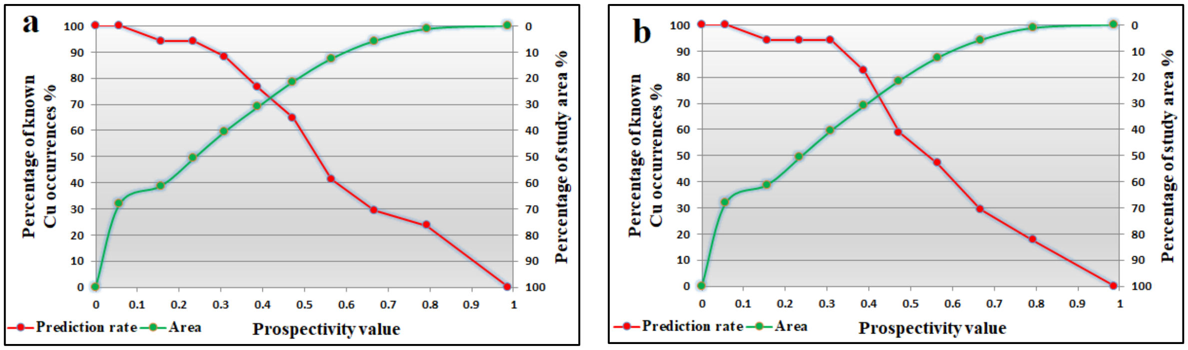

Figure 15. P-A plot for produced models by combination of a) interpolated values of GMPI, fault density, distance to intrusive rocks and distance to argillic and phyllic alterations; b) SCB model of GMPI, fault density, distance to intrusive rocks and distance to argillic and phyllic alterations using geometric average

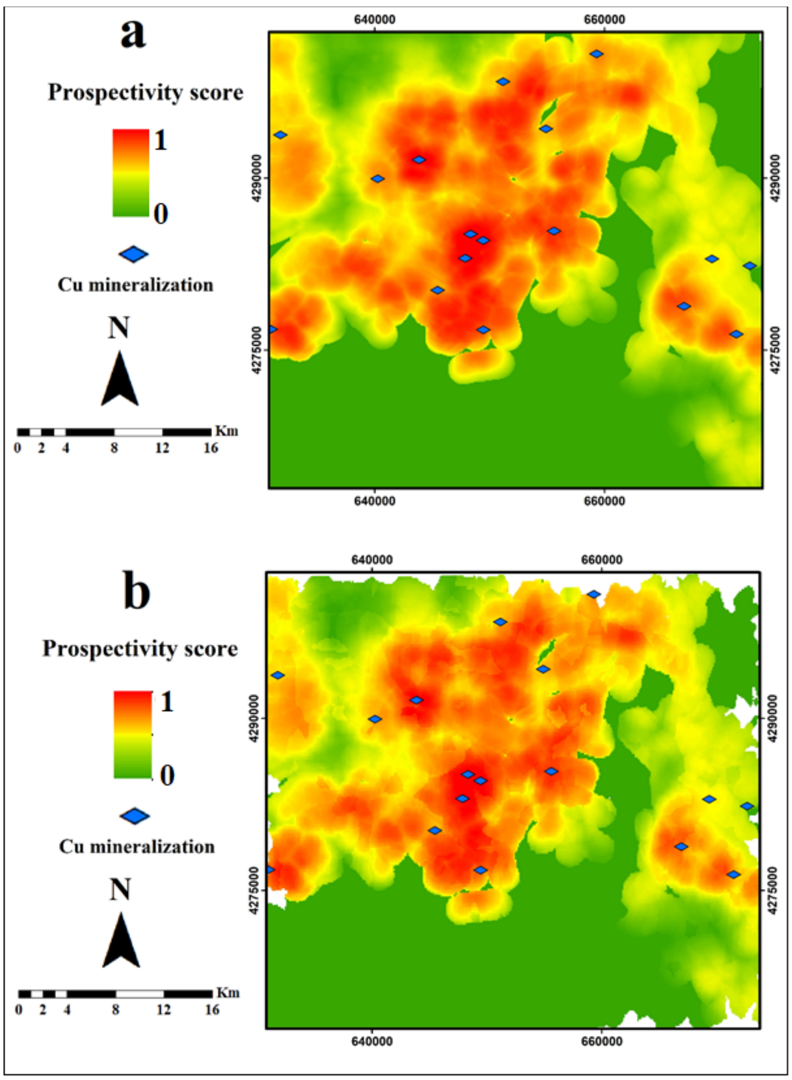

Figure 16. Mineral prospectivity model produced by combination of a) interpolated values of GMPI, fault density, distance to intrusive rocks and distance to argillic and phyllic alterations b;) SCB model of GMPI, fault density, distance to the intrusive rocks and distance to argillic and phyllic alterations using gamma fuzzy

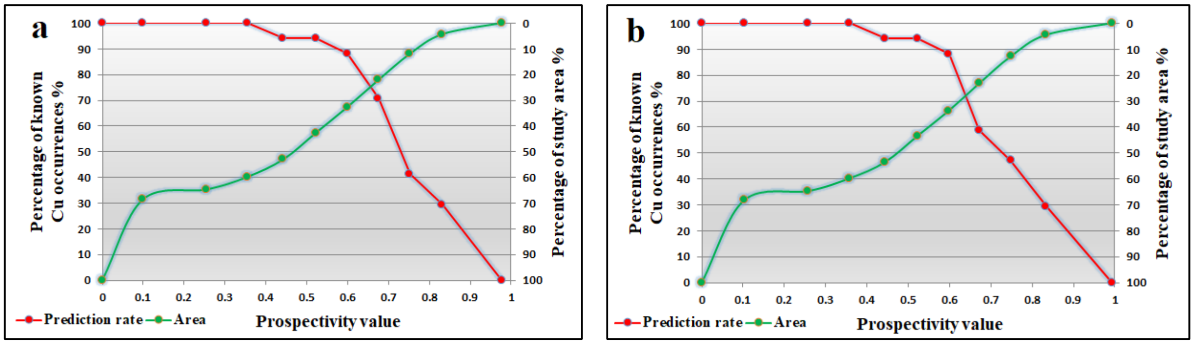

Figure 17. P-A plot for produced models by combination of a) interpolated values of GMPI, fault density, distance to intrusive rocks and distance to argillic and phyllic alterations b;) SCB model of GMPI, fault density, distance to the intrusive rocks and distance to argillic and phyllic alterations using gamma fuzzy

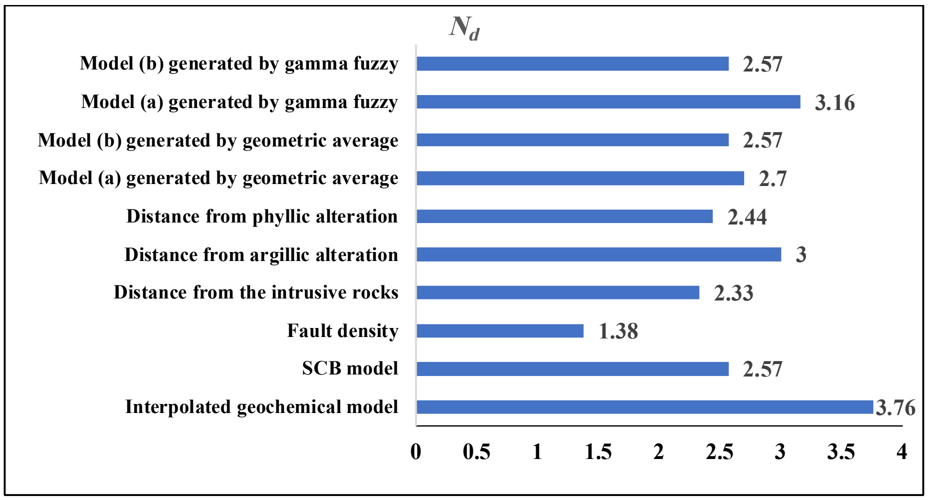

Figure 18. N_d for manufactured models

7. Discussions

The geochemical anomaly layer plays a crucial role in modeling the mineral potential of porphyry copper deposits, particularly at a regional scale. This study investigates the effects of two geochemical anomaly mapping methods on the MPM of porphyry copper deposits in the Varzaghan area. The findings indicate that the IDW model has a greater impact on the predictive accuracy of the final models compared to the SCB model, making it more efficient for MPM. One reason for the IDW model's effectiveness over the SCB model could be attributed to sampling density.

Various factors influence the distribution patterns of geochemical elements across different regions, making it essential to accurately analyze and identify significant geochemical signatures associated with the target deposits. In this context, the SFA method was employed to identify multi-element associations within the study area. The relationship between Cu, Mo, Au, and Bi in Factor 1, and the relationship between As and Sb in Factor 2, serve as reliable indicators for the exploration of porphyry copper deposits. Following the identification of these two factors, the GMPI was utilized to integrate information from both factors, creating a reliable geochemical layer for MPM. The results of the quantitative analysis demonstrated that this layer constitutes a strong geochemical signature for porphyry copper deposits in the region. Furthermore, the high prospectivity values associated with this layer are correlated with intrusive rocks and fault units in the area, underscoring the effectiveness of geochemical layers generated using SFA and GMPI.

The creation of efficient evidence layers, particularly the geochemical anomaly layer, enhances the predictive performance and reliability of prospectivity models in identifying promising areas. Analysis of the P-A plot and N_d values reveals that all layers, especially those related to geochemical anomalies, exhibit high efficiency. Subsequently, four final models were generated, all of which demonstrate strong predictive accuracy. Notably, the models integrating the geochemical anomaly evidence layer (interpolated model) with other layers show a higher prediction rate than the others. Additionally, the areas identified by these models exhibit a strong correlation with KMOs and intrusive units, highlighting their success in identifying exploration targets.

8. Conclusions

In the present study, weighted evidence layers of fault density, distance to intrusive rocks, geochemical anomaly, and distance to phyllic and argillic alterations were used to identify exploration targets by two MPM models, including the geometric average method and the fuzzy gamma operator. In this article, two methods for MPM were used because depending on the geological complexity, at least two prospective models should be created using two different methods to determine more precise exploration targets. MPM techniques based on these approaches can provide a rapid way of defining exploration targets for porphyry copper mineralization in the study area. According to the models obtained, the results of this research are as follows:

- Interpolation and SCB methods were employed to create the multi-element geochemical model. Evaluation results indicated that the interpolated model exhibited higher validity than the SCB method in this context. This outcome could be attributed to various factors, including sampling density. In areas with high sampling point density, interpolation methods like IDW may prove more effective due to their reliance on sample density.
- The approaches presented in this study effectively mitigate exploration biases by assigning fuzzy weights without relying on KMO locations or expert opinions.
- The four generated models demonstrated good agreement KMOs in the region, suggesting the utility of the diverse MPM models employed. This implies that both greenfield and brownfield exploration areas can benefit from the MPM approaches outlined in this article. In each region type, KMO locations can serve as test points for evaluating the generated model and for visualizing P-A plots.
- The findings of this study demonstrate that the prediction rate of KMOs applying fuzzy gamma operator prospectivity modeling for MPM is higher than that applying the geometric average prospectivity modeling method.

References

[1]. Ghezelbash, R., Maghsoudi, A., Daviran, M., & Yilmaz, H. (2019). Incorporation of principal component analysis, geostatistical interpolation approaches and frequency-space-based models for portraying the Cu-Au geochemical prospects in the Feizabad district, NW Iran. *Geochemistry, 79(2)*, 323-336.

[2]. Kashani, S. B. M., Abedi, M., & Norouzi, G. H. (2016). Fuzzy logic mineral potential mapping for copper exploration using multi-disciplinary geo-datasets, a case study in seridune deposit, Iran. *Earth Science Informatics, 9*, 167-181.

[3]. Parsa, M. (2021). A data augmentation approach to XGboost-based mineral potential mapping: an example of carbonate-hosted ZnPb mineral systems of Western Iran. *Journal of Geochemical Exploration, 228*, 106811.

[4]. Daviran, M., Maghsoudi, A., Cohen, D. R., Ghezelbash, R., & Yilmaz, H. (2020). Assessment of various fuzzy c-mean clustering validation indices for mapping mineral prospectivity: combination of multifractal geochemical model and mineralization processes. *Natural Resources Research, 29*, 229-246.

[5]. Zhang, S., Carranza, E. J. M., Xiao, K., Wei, H., Yang, F., Chen, Z., ... & Xiang, J. (2022). Mineral prospectivity mapping based on isolation forest and random forest: Implication for the existence of spatial signature of mineralization in outliers. *Natural Resources Research, 31(4)*, 1981-1999.

[6]. Hajihosseinlou, M., Maghsoudi, A., & Ghezelbash, R. (2024). Stacking: A novel data-driven ensemble machine learning strategy for prediction and mapping of Pb-Zn prospectivity in Varcheh district, west Iran. *Expert Systems with Applications, 237*, 121668.

[7]. Ghezelbash, R., Maghsoudi, A., & Carranza, E. J. M. (2019). Performance evaluation of RBF-and SVM-based machine learning algorithms for predictive mineral prospectivity modeling: integration of SA multifractal model and mineralization controls. *Earth Science Informatics, 12(3)*, 277-293.

[8]. Yousefi, M., & Hronsky, J. M. (2023). Translation of the function of hydrothermal mineralization-related focused fluid flux into a mappable exploration criterion for mineral exploration targeting. *Applied Geochemistry, 149*, 105561.

[9]. Yousefi, M., Lindsay, M. D., & Kreuzer, O. (2024). Mitigating uncertainties in mineral exploration targeting: Majority voting and confidence index approaches in the context of an exploration information system (EIS). *Ore Geology Reviews*, 105930.

[10]. Yousefi, M., & Nykänen, V. (2016). Data-driven logistic-based weighting of geochemical and geological evidence layers in mineral prospectivity mapping. *Journal of Geochemical Exploration, 164*, 94-106.

[11]. Ghezelbash, R., & Maghsoudi, A. (2018). Application of hybrid AHP-TOPSIS method for prospectivity modeling of Cu porphyry in Varzaghan district, Iran. *Scientific Quarterly Journal of Geosciences, 28(109)*, 33-42.

[12]. Shabani, A., Ziaii, M., Monfared, M. S., Shirazy, A., & Shirazi, A. (2022). Multi-Dimensional Data Fusion for Mineral Prospectivity Mapping (MPM) Using Fuzzy-AHP Decision-Making Method, Kodegan-Basiran Region, East Iran. *Minerals, 12(12)*, 1629.

[13]. Ghadiri-Sufi, E., & Yousefi, M. (2016). Combination of data-and knowledge-driven fuzzy approaches in mineral potential modeling for generating target areas. *Scientific Quarterly Journal of Geosciences, 25(98)*, 11-18.

[14]. Harris, J. R., Grunsky, E., Behnia, P., & Corrigan, D. (2015). Data-and knowledge-driven mineral prospectivity maps for Canada's North. *Ore Geology Reviews, 71*, 788-803.

[15]. Agha Seyyed Mirzabozorg, S. A., Abedi, M., & Ahmadi, F. (2023). Clustering of Areas Prone to Iron Mineralization in Esfordi Range based on a Hybrid Method of Knowledge-and Data-Driven Approaches. *Journal of Mineral Resources Engineering, 8(4)*, 1-26.

[16]. Farhadi, S., Tatullo, S., Konari, M. B., & Afzal, P. (2024). Evaluating StackingC and ensemble models for enhanced lithological classification in geological mapping. *Journal of Geochemical Exploration, 260*, 107441.

[17]. Lou, Y., & Liu, Y. (2023). Mineral prospectivity mapping of tungsten polymetallic deposits using machine learning algorithms and comparison of their performance in the Gannan region, China. *Earth and Space Science, 10(10)*, e2022EA002596.

[18]. Ghezelbash, R., & Esmailzadeh, M. (2021). Evaluation of machine learning algorithms for spatial predictive modeling of Au prospectivity. *Construction science and technology, 1(4)*, 53-64.

[19]. Pourgholam, M. M., Afzal, P., Adib, A., Rahbar, K., & Gholinejad, M. (2024). Recognition of REEs anomalies using an image Fusion fractal-wavelet model in Tarom metallogenic zone, NW Iran. *Geochemistry, 84(2)*, 126093.

[20]. Mokhtari, M., Hoseinzade, Z., & Shirani, K. (2020). A comparison study on landslide prediction through FAHP and Dempster–Shafer methods and their evaluation by P–A plots. *Environmental Earth Sciences, 79*, 1-13.

[21]. Rahimi, H., Abedi, M., Yousefi, M., Bahroudi, A., & Elyasi, G. R. (2021). Supervised mineral exploration targeting and the challenges with the selection of deposit and non-deposit sites thereof. *Applied Geochemistry, 128*, 104940.

[22]. Bigdeli, A., Maghsoudi, A., & Ghezelbash, R. (2024). A comparative study of the XGBoost ensemble learning and multilayer perceptron in mineral prospectivity modeling: a case study of the Torud-Chahshirin belt, NE Iran. *Earth Science Informatics, 17(1)*, 483-499.

[23]. Abedi, M., Kashani, S. B. M., Norouzi, G. H., & Yousefi, M. (2017). A deposit scale mineral prospectivity analysis: A comparison of various knowledge-driven approaches for porphyry copper targeting in Seridune, Iran. *Journal of African Earth Sciences, 128*, 127-146.

[24]. Riahi, S., Bahroudi, A., Abedi, M., Lentz, D. R., & Aslani, S. (2023). Application of data-driven multi-index overlay and BWM-MOORA MCDM methods in mineral prospectivity mapping of porphyry Cu mineralization. *Journal of Applied Geophysics, 213*, 105025.

[25]. Sabbaghi, H., & Tabatabaei, S. H. (2023). Data-driven logistic function for weighting of geophysical evidence layers in mineral prospectivity mapping. *Journal of Applied Geophysics, 212*, 104986.

[26]. Yousefi, M., Kamkar-Rouhani, A., & Carranza, E. J. M. (2012). Geochemical mineralization probability index (GMPI): a new approach to generate enhanced stream sediment geochemical evidential map for increasing probability of success in mineral potential mapping. *Journal of Geochemical Exploration, 115*, 24-35.

[27]. Daviran, M., Maghsoudi, A., Ghezelbash, R., & Pradhan, B. (2021). A new strategy for spatial predictive mapping of mineral prospectivity: Automated hyperparameter tuning of random forest approach. *Computers & Geosciences, 148*, 104688.

[28]. Mirzabozorg, S. A. A. S., & Abedi, M. (2023). Recognition of mineralization-related anomaly patterns through an autoencoder neural network for mineral exploration targeting. *Applied Geochemistry, 158*, 105807.

[29]. Saremi, M., Yousefi, M., & Yousefi, S. (2024). Separation of geochemical anomalies related to hydrothermal copper mineralization using staged factor analysis in Feizabad geological map.

[30]. Farhadi, S., Afzal, P., Boveiri Konari, M., Daneshvar Saein, L., & Sadeghi, B. (2022). Combination of machine learning algorithms with concentration-area fractal method for soil geochemical anomaly detection in sediment-hosted Irankuh Pb-Zn deposit, Central Iran. *Minerals, 12(6)*, 689.

[31]. Ghasemzadeh, S., Maghsoudi, A., Yousefi, M., & Mihalasky, M. J. (2022). Information value-based geochemical anomaly modeling: A statistical index to generate enhanced geochemical signatures for mineral exploration targeting. *Applied Geochemistry, 136*, 105177.

[32]. Bigdeli, A., Maghsoudi, A., & Ghezelbash, R. (2022). Application of self-organizing map (SOM) and

K-means clustering algorithms for portraying geochemical anomaly patterns in Moalleman district, NE Iran. *Journal of Geochemical Exploration, 233*, 106923.

[33]. Ghezelbash, R., Maghsoudi, A., & Carranza, E. J. M. (2019). Mapping of single-and multi-element geochemical indicators based on catchment basin analysis: Application of fractal method and unsupervised clustering models. *Journal of Geochemical Exploration, 199*, 90-104.

[34]. Yousefi, M., Carranza, E. J. M., & Kamkar-Rouhani, A. (2013). Weighted drainage catchment basin mapping of geochemical anomalies using stream sediment data for mineral potential modeling. *Journal of Geochemical Exploration, 128*, 88-96.

[35]. Maghsoudi, A., Yazdi, M., Mehrparto, M., & Vosoghi Abideni, M. (2009). Geochemical zonation in Mirkoh alimirza area, Arasbaran zone, NW Iran. *Geochimica et Cosmochimica Acta Supplement, 73*, A815.

[36]. Aghazadeh, M., Hou, Z., Badrzadeh, Z., & Zhou, L. (2015). Temporal–spatial distribution and tectonic setting of porphyry copper deposits in Iran: constraints from zircon U–Pb and molybdenite Re–Os geochronology. *Ore geology reviews, 70*, 385-406.

[37]. Hezarkhani, A., & Williams-Jones, A. E. (1998). Controls of alteration and mineralization in the Sungun porphyry copper deposit, Iran; evidence from fluid inclusions and stable isotopes. *Economic Geology, 93(5)*, 651-670.

[38]. Zarasvandi, A., Rezaei, M., Sadeghi, M., Lentz, D., Adelpour, M., & Pourkaseb, H. (2015). Rare earth element signatures of economic and sub-economic porphyry copper systems in Urumieh–Dokhtar Magmatic Arc (UDMA), Iran. *Ore geology reviews, 70*, 407-423.

[39]. Jamali, H., Dilek, Y., Daliran, F., Yaghubpur, A., & Mehrabi, B. (2010). Metallogeny and tectonic evolution of the Cenozoic Ahar–Arasbaran volcanic belt, northern Iran. *International Geology Review, 52(4-6)*, 608-630.

[40]. Ghezelbash, R., & Maghsoudi, A. (2018). Comparison of U-spatial statistics and C–A fractal models for delineating anomaly patterns of porphyry-type Cu geochemical signatures in the Varzaghan district, NW Iran. *Comptes Rendus Geoscience, 350(4)*, 180-191.

[41]. M. Mehrpartou, "Geological map of Varzaghan, scale 1: 1,000,000," *Geological survey of Iran,* 1993.

[42]. A. Maghsoudi, M. Yazdi, M. Mehrpartou, M. Vosoughi, and S. Younesi, "Porphyry Cu–Au mineralization in the Mirkuh Ali Mirza magmatic complex, NW Iran," *Journal of Asian Earth Sciences, vol. 79, pp.* 932-941, 2014.

[43]. Maghsoudi, A., Rahmani, M., & Rashidi, B. (2005). Gold deposits and indications of Iran.

[44]. Ghezelbash, R., Maghsoudi, A., & Carranza, E. J. M. (2020). Optimization of geochemical anomaly detection using a novel genetic K-means clustering (GKMC) algorithm. *Computers & Geosciences, 134*, 104335.

[45]. Ghezelbash, R., Maghsoudi, A., & Daviran, M. (2019). Prospectivity modeling of porphyry copper deposits: recognition of efficient mono-and multi-element geochemical signatures in the Varzaghan district, NW Iran. *Acta Geochimica, 38*, 131-144.

[46]. Bahri, E., Alimoradi, A., & Yousefi, M. (2021). Mineral Potential Modeling of Porphyry Copper Deposits using Continuously-Weighted Spatial Evidence Layers and Union Score Integration Method. *Journal of Mining and Environment, 12(3)*, 743-751.

[47]. Hezarkhani, A. (2006). Petrology of the intrusive rocks within the Sungun porphyry copper deposit, Azerbaijan, Iran. *Journal of Asian Earth Sciences, 27(3)*, 326-340.

[48]. Yousefi, M., Barak, S., Salimi, A., & Yousefi, S. (2023). Should geochemical indicators be integrated to produce enhanced signatures of mineral deposits? A discussion with regard to exploration scale. *Journal of Mining and Environment, 14(3)*, 1011-1018.

[49]. Lowell, J. D., & Guilbert, J. M. (1970). Lateral and vertical alteration-mineralization zoning in porphyry ore deposits. *Economic geology, 65(4)*, 373-408.

[50]. Pour, A. B., & Hashim, M. (2012). The application of ASTER remote sensing data to porphyry copper and epithermal gold deposits. *Ore geology reviews, 44*, 1-9.

[51]. Yousefi, M., & Carranza, E. J. M. (2015). Geometric average of spatial evidence data layers: a GIS-based multi-criteria decision-making approach to mineral prospectivity mapping. *Computers & Geosciences, 83*, 72-79.

[52]. Bahri, E., Alimoradi, A., & Yousefi, M. (2023). Investigating the performance of continuous weighting functions in the integration of exploration data for mineral potential modeling using artificial neural networks, geometric average and fuzzy gamma operators. *International Journal of Mining and Geo-Engineering, 57(4)*, 405-412.

[53]. Zhang, N., & Zhou, K. (2015). Mineral prospectivity mapping with weights of evidence and fuzzy logic methods. *Journal of Intelligent & Fuzzy Systems, 29(6)*, 2639-2651.

[54]. Li, H., Li, X., Yuan, F., Jowitt, S. M., Zhang, M., Zhou, J., ... & Wu, B. (2020). Convolutional neural network and transfer learning based mineral prospectivity modeling for geochemical exploration of Au mineralization within the Guandian–Zhangbaling area, Anhui Province, China. *Applied Geochemistry, 122*, 104747.

[55]. Saremi, M., Yousefi, S., & Yousefi, M. (2024). Combination of Geochemical and Structural Data to

Determine Exploration Target of Copper Hydrothermal Deposits in Feizabad District. *Journal of Mining and Environment, 15(3)*, 1089-1101.

[56]. Ghasemzadeh, S., Maghsoudi, A., Yousefi, M., & Mihalasky, M. J. (2019). Stream sediment geochemical data analysis for district-scale mineral exploration targeting: Measuring the performance of the spatial U-statistic and CA fractal modeling. *Ore Geology Reviews, 113*, 103115.

[57]. Afzal, P., Mirzaei, M., Yousefi, M., Adib, A., Khalajmasoumi, M., Zarifi, A. Z., ... & Yasrebi, A. B. (2016). Delineation of geochemical anomalies based on stream sediment data utilizing fractal modeling and staged factor analysis. *Journal of African Earth Sciences, 119*, 139-149.

[58]. Yilmaz, H., Yousefi, M., Parsa, M., Sonmez, F. N., & Maghsoodi, A. (2019). Singularity mapping of bulk leach extractable gold and− 80# stream sediment geochemical data in recognition of gold and base metal mineralization footprints in Biga Peninsula South, Turkey. *Journal of African Earth Sciences, 153*, 156-172.

[59]. Hoseinzade, Z., Mokhtari, A. R., & Zekri, H. (2018). Application of radial basis function in the analysis of irregular geochemical patterns through spectrum-area method. *Journal of Geochemical Exploration, 194. https://doi.org/10.1016/j.gexplo*.2018.09.002

[60]. Hajihosseinlou, M., Maghsoudi, A., & Ghezelbash, R. (2024). Intelligent mapping of geochemical anomalies: Adaptation of DBSCAN and mean-shift clustering approaches. *Journal of Geochemical Exploration, 258*, 107393.

[61]. Hoseinzade, Z., & Mokhtari, A. R. (2017). A comparison study on detection of key geochemical variables and factors through three different types of factor analysis. *Journal of African Earth Sciences, 134*, 557-563.

[62]. Saadati, H., Afzal, P., Torshizian, H., & Solgi, A. (2020). Geochemical exploration for lithium in NE Iran using the geochemical mapping prospectivity index, staged factor analysis, and a fractal model. *Geochemistry: Exploration, Environment, Analysis, 20(4)*, 461-472.

[63]. Wu, R., Chen, J., Zhao, J., Chen, J., & Chen, S. (2020). Identifying geochemical anomalies associated with gold mineralization using factor analysis and spectrum–area multifractal model in Laowan District, Qinling-Dabie Metallogenic Belt, Central China. *Minerals, 10(3)*, 229.

[64]. Meigoony, M. S., Afzal, P., Gholinejad, M., Yasrebi, A. B., & Sadeghi, B. (2014). Delineation of geochemical anomalies using factor analysis and multifractal modeling based on stream sediments data in Sarajeh 1: 100,000 sheet, Central Iran. *Arabian Journal of Geosciences, 7*, 5333-5343.

[65]. Yousefi, M., Kamkar-Rouhani, A., & Carranza, E. J. M. (2014). Application of staged factor analysis and logistic function to create a fuzzy stream sediment geochemical evidence layer for mineral prospectivity mapping. *Geochemistry: Exploration, Environment, Analysis, 14(1)*, 45-58.

[66]. Aryafar, A., Yousefi, S., Khosravi, V., & Khorashadi, M. (2020). Using stepwise factor analysis (SFA) and geochemical mineralization probability index (GMPI) in order to intensify the geochemical anomalies associated with vein-type copper mineralization in Kardgan 1: 100000 sheet, East of Iran. *Journal of Mining Engineering, 15(47)*, 1-13.

[67]. Afzal, P., Yusefi, M., Mirzaie, M., Ghadiri-Sufi, E., Ghasemzadeh, S., & Daneshvar Saein, L. (2019). Delineation of podiform-type chromite mineralization using geochemical mineralization prospectivity index and staged factor analysis in Balvard area (SE Iran). *Journal of Mining and Environment, 10(3)*, 705-715.

[68]. Yousefi, M., & Carranza, E. J. M. (2015). Prediction–area (P–A) plot and C–A fractal analysis to classify and evaluate evidential maps for mineral prospectivity modeling. *Computers & Geosciences, 79*, 69-81.

[69]. Hoseinzade, Z., Zavarei, A., & Shirani, K. (2021). Application of prediction–area plot in the assessment of MCDM methods through VIKOR, PROMETHEE II, and permutation. *Natural Hazards, 109*, 2489-2507.

[70]. Roshanravan, B., Aghajani, H., Yousefi, M., & Kreuzer, O. (2019). An improved prediction-area plot for prospectivity analysis of mineral deposits. *Natural Resources Research, 28*, 1089-1105.

مدلسازی پتانسیل معدنی مس پورفیری با استفاده از توابع لجستیکی در منطقه ورزقان، شمال کمان ماگمایی ارومیه-دختر

مبین صارمی[۱]، عباس مقصودی[۱*]، رضا قزلباش[۲]، مهیار یوسفی[۳] و اردشیر هزارخانی[۱]

۱. گروه مهندسی معدن، دانشکده مهندسی معدن، دانشگاه صنعتی امیرکبیر، ایران
۲. دانشکدگان فنی، دانشکده مهندسی معدن، دانشگاه تهران، ایران
۳. گروه مهندسی معدن، دانشکده فنی و مهندسی، دانشگاه ملایر

ارسال ۲۰۲۴/۰۷/۲۰، پذیرش ۲۰۲۴/۰۸/۳۰

* نویسنده مسئول مکاتبات: a.maghsoudi@aut.ac.ir

چکیده:

مدلسازی پتانسیل معدنی فرآیندی چندمرحله‌ای و پیچیده است که با تحلیل و تلفیق مجموعه داده‌های اکتشافی مختلف، منطقه تحت پوشش عملیات اکتشافی را محدود کرده و به شناسایی مناطق امیدبخش می‌پردازد. در مطالعه حاضر، برای تعیین مناطق امیدبخش کانی‌سازی مس پورفیری در ناحیه ورزقان واقع در شمال غرب ایران، لایه‌های شاهد اکتشافی مختلف بر اساس مدل مفهومی این کانسارها تهیه شد. این لایه‌ها شامل چگالی گسل، فاصله از توده نفوذی، آنومالی ژئوشیمیایی چندمتغیره، و فاصله از دگرسانی‌های فیلیک و آرژیلیک بودند. نقشه‌های ناهنجاری ژئوشیمیایی، که به عنوان یکی از مؤثرترین لایه‌ها شناخته شدند، از طریق تحلیل فاکتوری مرحله‌ای و شاخص احتمال کانی‌سازی ژئوشیمیایی ساخته شدند. سایر لایه‌ها نیز تولید و با استفاده از یک تابع لجستیک بهینه، به بازه ۰ تا ۱ انتقال داده شدند. در نهایت، برای تلفیق لایه‌های شاهد وزن‌دار، از عملگر گامای فازی و روش میانگین هندسی استفاده شد. برای ارزیابی مدل‌های تولید شده، از شاخص چگالی نرمال شده و نمودار نرخ پیش‌بینی-مساحت استفاده گردید. یافته‌های این پژوهش نشان می‌دهند که مدل‌های ساخته شده دارای اعتبار قابل‌توجهی هستند و می‌توانند به طور موثر برای برنامه‌ریزی عملیات‌های اکتشافی آتی مورد استفاده قرار گیرند.

کلمات کلیدی: کانسارهای مس پورفیری، ژئوشیمی رسوبات آبراهه‌ای، تحلیل فاکتوری مرحله‌ای ، شاخص احتمالی کانی‌سازی ژئوشیمیایی، مدلسازی پتانسیل معدنی.